Int. J. Heat Mass Transfer. Vol. 35, No. 2, pp. 279–294, 1992
Printed in Great Britain

0017–9310/92 $5.00+0.00

Reflux condensation heat transfer inside a closed thermosyphon†

U. GROSS
Institut für Thermodynamik und Wärmetechnik, Universität Stuttgart, Pfaffenwaldring 6, 7000 Stuttgart 80, Germany

(*Received* 9 *September* 1991)

Abstract—A survey is given on condensation heat transfer inside a two-phase thermosyphon including a detailed description of fluid flow as well as a review of published experimental and theoretical investigations. A total of 2889 data points derived from 18 research works has been evaluated covering wide ranges of thermal and geometrical parameters: 10 different working fluids, saturation temperature ($14°C \leqslant t_s \leqslant 340°C$), pressure ($0.04 \leqslant p \leqslant 39.5$ bar), inside tube diameter ($14 \leqslant d \leqslant 66$ mm), length of cooling zone ($102 \leqslant L \leqslant 2450$ mm), and inclination angle ($0° \leqslant \varphi \leqslant 85°$). Correlations are proposed for condensation heat transfer inside a two-phase thermosyphon. Remaining deviations are due to effects of shear stress at the liquid–vapour interface, effects of non-condensable gases and effects of a partial flooding of the cooling zone in the case of superfilling the thermosyphon.

1. INTRODUCTION

A CLOSED two-phase thermosyphon (wickless heat pipe) consists of a tube which is closed at both ends and filled with a certain amount of a pure fluid. Usually a straight circular tube is used in a vertical or inclined position. A natural counter-current two-phase flow is forced inside with evaporation and condensation in the heated lower section and in the cooled upper section, respectively.

Condensation heat transfer inside a two-phase thermosyphon has been studied in a large number of theoretical and experimental investigations (see Table 1). Respective publications include:

- visual observations of the fluid flow (labelled as 'visual'),
- measurements of heat transfer coefficients ('α-data'),
- measurements of non-condensable gas effects ('inert'),
- correlations of heat transfer data ('α-corr'),
- analysis of shear stress effects due to vapour flow ('theory').

There are two surveys which illuminate the state of the art in the years 1973 [7] and 1981 [16]. The great amount of research work which has been done since that time (see Table 1) asks for a critical review of both the heat transfer data and the correlations. Therefore all the material from the open literature has been collected and classified with the aim to provide correlations for practical application (Groß [57]).

† Dedicated to Prof. Dr.-Ing. E. Hahne on the occasion of his 60th birthday.

2. DESCRIPTION OF FLUID FLOW

In the adiabatic steady state ($Q = 0$ W), the fluid inside the thermosyphon is in thermodynamic equilibrium with the saturation state at liquid level. The liquid below is subcooled to some amount due to the hydrostatic pressure head, whereas the vapour does not deviate significantly from saturation.

2.1. *Filmwise condensation*

The thermosyphon is brought into operation as soon as heat is removed from above, or as it is supplied from below. A driving temperature difference grows between saturation state (in the vapour space) and the now subcooled wall, where condensation is forced at nucleation sites. In the case of a wetting fluid, the wall will soon be covered by a thin liquid film which flows downwards, driven by gravity and retarded by viscosity.

Vertical tube. With the thermosyphon in vertical position the film flow is one-dimensional. Thickness and velocity of the film grow to maximum values at the lower end of the cooling zone. At a small film Reynolds number

$$Re = w_L \delta_L / \nu_l = Q/(\pi d \eta_l \Delta h_v) \quad (<5, \text{roughly}) \qquad (1)$$

the film flow is laminar with a smooth vapour-side interface. Heat is transferred by pure heat conduction across the film, which is subcooled to some amount.

Inclined tube. If the tube is tilted from vertical the liquid flow field becomes two-dimensional. Now the streamlines form curved paths, which discharge into the lower-most part of the tube's cross section where a thick stream of liquid flows axially downwards to the heating zone.

Wave formation. Wave formation is observed, e.g. refs. [13, 23, 36], at the interface if the film *Re* exceeds

NOMENCLATURE

Ar	Archimedes number, equation (5c)
d	inside tube diameter [m]
d_b	Laplace constant, $(\sigma/(\rho_l-\rho_v)g)^{0.5}$ [m]
d_{hydr}	hydraulic diameter [m]
f_i	dimensionless factors (f_p, f_φ, f_{wave})
Fr_b	bubbly-flow Froude number, $w_{vo}^2/(gd_b)$
Fr_{vo}	vapour-flow Froude number, $w_{vo}^2/(gd)$
g	acceleration of gravity [m s^{-2}]
Δh_v	latent heat of vaporization [J kg^{-1}]
L	length [m]
Nu	Nusselt number, equation (5b)
Nu^*	modified Nusselt number, equation (5a)
p	pressure [bar]
p^*	dimensionless pressure, $p/p_{critical}$
Pr	Prandtl number
Q	heat flow rate [W]
Re	film-flow Reynolds number, equation (1)
Re_φ	modified film Reynolds number, equation (8)
Re_{vo}	vapour-flow Reynolds number, $w_{vo}d/v_v$
t	temperature [°C]
ΔT	temperature difference [K]
w	mean velocity [m s^{-1}]
w_{vo}	superficial velocity, $Q/A_{cr}\Delta h_v\rho_v$ [m s^{-1}].

Greek symbols

α	heat transfer coefficient [W m^{-2} K^{-1}]
δ_L	film thickness at the lower end of the cooling zone [m]
δ_v	characteristic length, equation (5d) [m]
η	dynamic viscosity [kg m^{-1} s^{-1}]
λ	thermal conductivity [W m^{-1} K^{-1}]
ν	kinematic viscosity [m^2 s^{-1}]
ξ	dimensionless friction factor, equation (20)
ρ	density [kg m^{-3}]
σ	surface tension [N m^{-1}]
τ	shear stress at the liquid–vapour interface, equation (20) [N m^{-2}]
τ^*	dimensionless shear stress, equation (21)
φ	inclination angle vs vertical direction [deg].

Subscripts

cr	cross section
flood	flooding limit
i	inside
l	liquid
o	outside
v	vapour
s	saturation
trans	transition
w	wall.

a limiting value of about $Re = 5$. Damping effects by viscosity and smoothing effects by surface tension are no longer able to suppress wavy structures. Heat transfer across the, still laminar, film is improved by the wave formation due to a reduction of the effective thickness of the laminar film between the wave crests.

Turbulence. Turbulent structures within the film are more and more able to develop, if thickness and velocity of the film are further increased, or if viscosity is decreased. Finally the film flow becomes turbulent. The governing heat transfer mechanism is now due to turbulent exchange processes which exceed the molecular heat conduction, by far.

Shear stress, entrainment, flooding. Mass conservation inside the thermosyphon calls for identical mass flow rates of liquid and vapour, with the two phases in counter-current flow. If shear stress at the liquid–vapour interface grows large, liquid particles may be entrained from the liquid film. These droplets are then transported by the vapour flow in upward direction and finally deposited on the film surface [53]. Heat transfer coefficients are caused to decrease. At extremely high vapour velocities the counter flow of liquid and vapour becomes unstable and flooding of the cooling zone may occur. The liquid is now completely held in the upper part of the tube, whereas the heating zone goes dry. Large heat flow rate, small tube diameter, small latent heat of vaporization (especially at high pressure), and small vapour density (especially at extremely small pressure) yield those large vapour velocities ($w_{vo} = Q/A_{cr}\Delta h_v\rho_v$) which bring a thermosyphon to the flooding limit.

Non-condensable gases. Non-condensable gases are collected in the most upper part of the thermosyphon, forming an additional transport resistance due to mass diffusion. Condensation heat transfer is now restricted to a, more or less, small part of the cooling zone surface.

2.2. *Dropwise condensation*

Dropwise condensation, with its extremely favourable rates of heat transfer, has been visually observed in a thermosyphon [3, 13]. It is only found if a fluid with strong cohesion (e.g. water) is used in combination with a cooling surface, to which adhesion forces are small, and thus no wetting occurs. Such conditions can be favoured by gold plating the surface or by mixing some promotor (oil, oleic acid and others) with the fluid, which is thought to be held at the surface but not washed away. Dropwise condensation inside a thermosyphon has been realized only exceptionally for more [37], or less [3], long times.

Table 1. Theoretical and experimental investigations of cooling zone heat transfer inside a two-phase thermosyphon

1967	Larkin [1]			experi.	visual			
1968	Stoyanov [2]			experi.			α-data	α-corr
1971	Larkin [3]			experi.	visual		α-data	
1972	Andreev [4, 5]			experi.			α-data	
1973	Gorbis/Savchenkov [6]		theory	experi.		inert		
	Japikse [7]	survey						
1978	Semena/Kiselev [8]			experi.			α-data	α-corr
	Suematsu *et al.* [9]		theory	experi.			α-data	
1979	Alabovsky/Bezrodnyi/Moklyak [10]			experi.			α-data	
	Imura *et al.* [11]			experi.	visual		α-data	
	Kiselev *et al.* [12]			experi.			α-data	
1980	Andros [13]			experi.	visual		α-data	α-corr
	Hirshberg [14]		theory	experi.			α-data	
	Harada *et al.* [15]			experi.			α-data	
1981	ESDU [16]	survey						α-corr
	Ho/Tien [17]			experi.			α-data	
	Larkin [18]			experi.			α-data	
	Shiraishi/Kikuchi/Yamanishi [19]			experi.			α-data	
	Spendel [20]		theory					
1982	Andros/Florschuetz [21]			experi.			α-data	
	Mirmov/Portnov/Belyakova [22]			experi.		inert	α-data	
	Takuma/Maezawa/Tsuchida [23]		theory	experi.	visual		α-data	
1983	Bezrodnyi/Moklyak [24]			experi.			α-data	α-corr
	Groß [25]			experi.			α-data	
	Mirmov/Belyakova [26]			experi.		inert	α-data	
1984	Chen/Reed/Tien [27]		theory	experi.		inert	α-data	
	Seban/Faghri [28]		theory					
	Takuma/Maezawa/Tsuchida [29]		theory	experi.		inert		
	Spendel [30]		theory					
	Hijikata/Chen/Tien [31]		theory			inert		
1985	Groß/Hahne [32]			experi.			α-data	
	Spendel [33]		theory					
1986	Bezrodnyi/Moklyak [34]			experi.			α-data	α-corr
	Groß/Hahne [35]			experi.			α-data	α-corr
	Takuma/Maezawa/Tsuchida [36]		theory	experi.	visual			
	Xin/Xia [37]			experi.			α-data	
1987	Appel [38]			experi.			α-data	
	Ma/Liu/Fung [39]			experi.	visual		α-data	
	Groß/Hahne [40, 41]			experi.			α-data	α-corr
	Hahne/Groß/Barthau [42]			experi.	visual			
	Kobayashi/Matsumoto [43]		theory	experi.	visual	inert		
	Rösler/Groll [44]			experi.				
1988	Peterson/Tien [45]			experi.		inert		
1989	Faghri/Chen/Morgan [46]		theory	experi.			α-data	
	Peterson/Tien [47]		theory			inert		
1990	Assad/Konev [48]		theory					
	Gerner/Tien [49]			experi.			α-data	
	Ma *et al.* [50]		theory	experi.			α-data	
	Niro/Radaelli/Andreini [51]			experi.			α-data	
	Tanaka *et al.* [52]			experi.			α-data	
	Fukano/Kadoguchi/Tien [53]		theory	experi.	visual		α-data	
	Sun/Zhao/Zhang [54]		theory					
1991	Peterson *et al.* [55]			experi.		inert		
	Zhou/Collins [56]			experi.		inert		
	Groß [57]	survey						α-corr

3. THEORETICAL APPROACH FOR LAMINAR FILM FLOW AND HEAT TRANSFER

There are a number of theoretical investigations in which filmwise condensation heat transfer inside a thermosyphon has been studied with, and without, consideration of effects due to the counter-current vapour flow. The mean heat transfer coefficient is defined as

$$\alpha = Q/(\pi d L(t_s - t_w)) \quad (2)$$

with t_w as the arithmetically averaged wall temperature in the cooling zone and t_s as the saturation temperature in the vapour space.

3.1. *Assumption of a stagnant vapour*

Vertical tube. The classical solution for laminar film condensation at a vertical surface has been provided by Nusselt [59]. He considered boundary conditions which are mathematically simple, but difficult to realize in practice. For the assumptions of negligible

shear stress at the liquid–vapour interface, negligible subcooling of the liquid film, constant temperature difference $\Delta T = t_s - t_w$ between saturation state and wall surface, and others (see ref. [59]), the mean heat transfer coefficient is obtained as

$$\alpha = 0.943(g(\rho_l - \rho_v)\Delta h_v \lambda_l^3/(\nu_l L \Delta T))^{1/4}. \quad (3)$$

Equation (3) can be brought into a dimensionless form (with $\Delta T = Q/(\alpha \pi d L)$)

$$Nu^* = 0.925 Re^{-1/3} \quad (4)$$

by introducing the modified Nusselt number Nu^* as

$$Nu^* = Nu\, Ar^{-1/3} = \alpha \delta_v / \lambda_l \quad (5a)$$

and

$$Nu = \alpha \delta_L / \lambda_l \quad (5b)$$

$$Ar = (g\delta_L^3/\nu_l^2)(\rho_l - \rho_v)/\rho_l \quad (5c)$$

$$\delta_v = ((\nu_l^2/g)\rho_l/(\rho_l - \rho_v))^{1/3}. \quad (5d)$$

Inclined tube. Heat transfer outside an inclined tube has been first analysed by Hassan and Jakob [60] applying Nusselt's assumptions. They obtained an expression for an infinitely long tube, which may be written as

$$Nu^* = 0.651 Re^{-1/3}(d/(L \sin \varphi))^{-1/3}. \quad (6)$$

The error due to finite tube length keeps below 10% for $[\tan \varphi L/d] > 2.5$ (i.e. if inclination angle φ and aspect ratio L/d are large). Equations (4) and (6), for vertical and inclined tubes respectively can be transformed into a common expression

$$Nu^* = 0.925 Re_\varphi^{-1/3} \quad (7)$$

if an inclination factor f_φ is introduced [35, 40] to obtain the modified Reynolds number

$$Re_\varphi = Re\, f_\varphi \quad (8)$$

with

$$f_\varphi = 1$$

for vertical tubes ($\varphi = 0°$)

$$f_\varphi = 2.87(d/(L \sin \varphi))$$

for inclined tubes with $\varphi > 10°$ (approximately for aspect ratios L/d which are typical for thermosyphons).

3.2. *Laminar flow of vapour*

In most practical cases Nusselt's assumptions are not fully valid, due to (at least) a finite shear stress at the liquid–vapour interface. This has to be considered as a boundary condition in the solution of the differential equation of momentum for the film flow. The shear stress effect is to increase film thickness and to decrease heat transfer coefficients.

Spendel [20, 30, 33] considered film condensation inside a thermosyphon under the effect of a variable shear stress along the cooling zone. The film is assumed to be laminar and smooth (just like in Nusselt's theory) but now a two-dimensional (axial/radial) laminar vapour flow is superposed. Numerical results show that reverse flow of vapour (downwards) may occur at the uppermost end of the tube. Mean heat transfer coefficients are in reasonably good agreement with Nusselt's theory. The remaining deviations are found to increase slightly if the vapour-flow Froude number ($Fr_{vo} = w_{vo}^2/(gd)$) is raised: less than 1% for $Fr_{vo} < 100$ and 3% (for about $Fr_{vo} = 500$) as the maximum in the cases considered.

3.3. *Turbulent flow of vapour*

In practice, the vapour flow inside a thermosyphon is rather turbulent than laminar, and boundary conditions are more complicated due to wavyness of the phase interface and droplet deposition on the film.

Smooth liquid–vapour interface. Takuma *et al.* [23], Chen *et al.* [27], Assad and Konev [48], Ma *et al.* [50] and Suematsu *et al.* [9] presented models for laminar film condensation with laminar or turbulent vapour flow and a smooth interface in between. Shear stresses are calculated from Fanning friction factors for laminar and turbulent pipe flow respectively. A decrease of the axial vapour velocity due to condensation is under consideration. The results show diminishing effects on heat transfer for small vapour velocities (e.g. with methanol [27], ethanol [23]; $Fr_{vo} \leqslant 1$). However, a strong effect is found if the velocity is large (e.g. with water, especially at low temperatures) [27]. This has been demonstrated by differences between the Nusselt numbers from the measurement and from Nusselt's theory: the first one is smaller by about 10% ($t_s = 100°C$; $Fr_{vo} = 5$) and 25% ($t_s = 40°C$; $Fr_{vo} = 340$). Results by Suematsu *et al.* show deviations between 3% (for $Fr_{vo} = 100$) and 8% (for $Fr_{vo} = 400$).

Additional effect of wave formation. Heat transfer resistance across the film is reduced by wave formation, e.g. see ref. [14]. Seban and Faghri [28] presented a one-dimensional model for laminar-wavy film condensation with laminar or turbulent vapour flow applying friction factors due to Henstock and Hanratty [61]. The governing equations have been solved numerically for operating conditions, which are similar to those used by Ho and Tien [17] in their experiments. Agreement with the simple Nusselt solution proves to be good (for $Fr_{vo} < 25$). The comparisons are supplemented by selected cases where the deviations grow large:

(a) extremely small tube diameter ($d = 2.4$ mm),

(b) extremely large temperature difference ($\Delta T = 1000$ K), and

(c) extremely large liquid viscosity (100 times the value of methanol).

Development of the wavy-film model [28] has been carried out by Faghri *et al.* [46] by consideration of film condensation inside an annular thermosyphon, with cooling at both the inside and the outside cylindric walls. The result is the same: shear effects are

negligibly small in the whole range of experiments with R113 and acetone which exceed the flooding limit [46].

The counteracting effects of wavyness (increase of heat transfer coefficient) and shear stress (decrease) upon each other have been studied by Takuma *et al.* [36] in a numerical study. The former effect is found to dominate in almost all the cases besides water at low temperature.

Additional effect of droplet deposition. Very recently Fukano *et al.* [53] presented a semi-analytical investigation where the effects of wavyness and shear stress were considered together with an additional effect due to the deposition of entrained droplets on the film surface. The latter effect is to decrease the heat transfer coefficients, especially in the most upper section of the cooling zone where film thickness is small.

4. EXPERIMENTAL WORK

4.1. *Survey*

Lots of experimental investigations have been carried out in the course of the past twenty years (Table 1). In almost all of the studies temperature distributions and heat transfer coefficients have been determined. These are supplemented by a number of experimental investigations of the flow structure [36, 42, 44] and of non-condensable gas distributions [29, 31, 43, 45, 55, 56] in the vapour space.

Table 2 gives major parameters of the experimental investigations using all the published heat transfer data, except those where the reported material is not complete enough for a further evaluation of data. In such cases there is, typically, a lack of experimental details or of the definition of dimensionless numbers. For each of the complete data sets, Table 2 includes information about working fluid and number of data points, supplemented by the respective ranges of diameter and length of the cooling zone, saturation temperature and corresponding pressure. Most of the experiments have been carried out inside a vertical thermosyphon except those of Larkin [18] ($\varphi = 85°$), Hirshberg [14] ($0° \leqslant \varphi \leqslant 90°$) as well as Groß [25, 32] ($0° \leqslant \varphi \leqslant 60°$) and [35] ($0° \leqslant \varphi \leqslant 80°$).

The last column of Table 2 is thought to give an idea of how close to practical operating conditions the experiments have been carried out. The designed operating point of a thermosyphyon will be as close as possible to the flooding limit, but keeping a sufficient distance to avoid flooding at small perturbations from the designed point. For all the data points, the actual vapour velocity ($w_{vo} = Q/(A_{cr}\Delta h_v \rho_v)$) has been related to the velocity required for flooding as predicted from Imura's equation [62]

$$w_{flood} = 0.64\,(\rho_l/\rho_v)^{0.13}(\sigma g(\rho_l - \rho_v)/\rho_v^2)^{0.25}. \quad (9)$$

The respective ranges of w_{vo}/w_{flood} given in the last column of Table 2 show that the flooding limit (i.e. $w_{vo}/w_{flood} = 100\%$) has been exceeded in many experiments.

4.2. *Correlations*

A number of correlations for condensation heat transfer inside a thermosyphon have been suggested (see Table 1) which take into account the special effects of wave formation and inclination. All of them are based on Nusselt's theory.

Consideration of wave formation. Measured heat transfer coefficients are usually compared with predicted ones from Nusselt's theory (equations (3) and (4)) and mostly they are found to be larger due to wave formation. Various suggestions can be found in the literature for 'wave factors' (for this, see ref. [40]) which consider the observed enhancement of heat transfer, for example as a constant factor ($f_{wave} = 1.28$, McAdams) or as a function of film Re ($f_{wave} = 0.8Re^{0.11}$, Zazuli; $f_{wave} = 0.956Re^{0.083}$, Uehara).

Special wave factors for thermosyphon experiments have been correlated by Andros [13] to predict his own experimental results:

for circular cross section

$$f_{wave} = 0.842Re^{0.033} \quad \text{with R113}, 8 < Re < 100 \quad (10)$$

for annular cross section

$$f_{wave} = 0.895Re^{0.128} \quad \text{with R113}, 10 < Re < 75 \quad (11)$$

$$f_{wave} = 0.960Re^{0.122} \quad \text{with ethanol}, 2 < Re < 8. \quad (12)$$

Consideration of tube inclination. If the tube is tilted from the vertical position ($\varphi = 0°$), film thickness is no longer axisymmetric and mean heat transfer coefficients increase. Semena and Kiselev [8] suggest the following empirical equation for the range $0° \leqslant \varphi \leqslant 75°$:

$$Nu^*/Nu^*_{eq.4} = 1 + 0.074(\sin\varphi\, L/d)^{0.7}. \quad (13)$$

Stoyanov [2] obtained an equation from his experiments with ammonia inside a thermosyphon cooled from the front surface ($d = 30$ mm, $L_{total} = 5$ m, $t_s = 100°C$, $0° \leqslant \varphi \leqslant 75°$)

$$Nu^*/Nu^*_{eq.4} = 1 + 0.26(\sin\varphi)^{0.5}. \quad (14)$$

Suggestion by ESDU [16]. The ESDU organization provided a compilation for the design of thermosyphons where the following correlations are recommended for prediction of the cooling zone heat transfer:

(a) Laminar film flow, vertical tube ($Re < Re_{trans} = 325$, $\varphi = 0°$) (Nusselt's equation [59] for mean values along a vertical surface)

$$Nu^* = 0.925Re^{-1/3}. \quad (4)$$

It is mentioned in ref. [16] that this equation may yield too small heat transfer coefficients due to wave formation.

(b) Laminar film flow, inclined tube ($\varphi = 85°$)

Table 2. Experimental investigations of filmwise condensation inside a thermosyphon

Fluid Author	Number of points	d (mm)	L (mm)	t_s (°C)	p (bar)	How close to flooding? w_{vo}/w_{flood} (%)
Water						
[9]	27	17–22	250–290	(≤180)	(≤10.0)	‡
[15]	52	45	2450	50–100	0.12–1.01	23–100
[18]	4	24	575	39–94	0.06–0.8	8–17
[19]	29	37	450	32–60	0.04–0.19	1–16
[24, 34]	71	18–66	(390–1335)	100–165	1.0–7.0	5–100
[27]	16	14	940	100	1.0	1–30
[50]	138	20	588	100–120	1.0–2.0	6–100
Dowtherm A						
[9]	36	17	250	(≤340)	(≤4.6)	‡
Acetone						
[46]	14	45/29†	219	‡	‡	(≤100)
Methanol						
[17]	6	24	305	62–67	0.93–1.06	40–52
[27]	16	14	940	66	1.0	2–89
Ethanol						
[13]	133	51/35†	102–191	21–58	0.06–0.42	1–14
[14]	9	27	762	34–57	0.14–0.41	38–100
[19]	20	37	450	32–45	0.11–0.22	1–52
[24, 34]	155	18–36	(390–1335)	78–153	1.0–10.5	7–100
[50]	20	62/56†	350	78	1.0	36–77
R11						
[10]	169	12–36	(200–1000)	23–89	1.0–6.5	3–100
[24, 34]	141	18–36	(390–1335)	23–105	1.0–9.15	11–100
[38]	23	21	400	37–120	1.62–12.22	9–44
R113						
[13]	190	51/35†	102–191	22–83	0.39–2.87	1–19
[13, 21]	62	27	762	25–88	0.44–3.25	5–100
[14]	52	27	152–762	26–74	0.46–2.26	8–100
[19]	9	37	450	32	0.58	1–25
[34]	28	18	(390–1335)	59–121	1.5–7.0	23–100
[46]	18	45/29†	219	‡	‡	(≤100)
R22						
[18]	24	24	575	14–68	7.83–28.54	29–92
R115						
[25, 32]	431	40	765	56–80	19.16–31.13	14–100
R13B1						
[35]	996	40	765	16–67	13.00–39.49	7–100

† Annular thermosyphon with d_o/d_i.
‡ No information.
( ) No detailed information, only the range has been published.

(Nusselt's equation for mean values along a horizontal tube)

$$Nu^* = 0.651(L/d)^{1/3}\, Re^{-1/3}. \quad (15)$$

(c) Turbulent film flow, vertical tube ($Re \geqslant 325$) (according to McAdams)

$$Nu^* = 0.0134 Re^{0.4}. \quad (16)$$

5. RESULTS AND DISCUSSION

5.1. *Diagrams*

All the experimental data (Table 2) have been evaluated and plotted in double logarithmic diagrams as Nu^* vs Re_φ. The results are given separately in Figs. 1–7 for the various fluids. Three straight lines are included which represent correlations for heat transfer:

(a) In the laminar range, Nusselt's theory

$$Nu^* = 0.925 Re_\varphi^{-1/3}. \quad (7)$$

(b) In the laminar-wavy range ($2 < Re_\varphi < 1333 \times Pr_l^{-0.96}$) following Uehara *et al.* [58]

$$Nu^* = 0.884 Re_\varphi^{-1/4}. \quad (17)$$

(c) In the turbulent range ($1333 Pr_l^{-0.96} < Re_\varphi$), also provided by Uehara *et al.*

$$Nu^* = 0.044 Pr_l^{2/5}\, Re_\varphi^{1/6}. \quad (18)$$

The figures for all the fluids, besides water, show that the data points follow equations (17) and (18), with a scatter which is pretty large in part.

Uncertainties in measurements? Deviations may be due to uncertainties in the measurements. Details of the measuring technique are missed in most of the experimental publications. Nevertheless there is some possibility to check whether a data point is uncertain or not. The maximum error in condensation heat

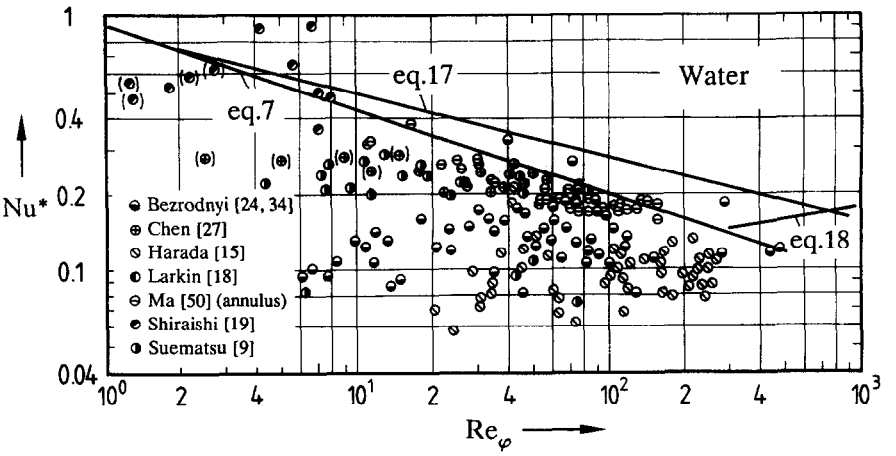

FIG. 1. Reflux condensation heat transfer with water.

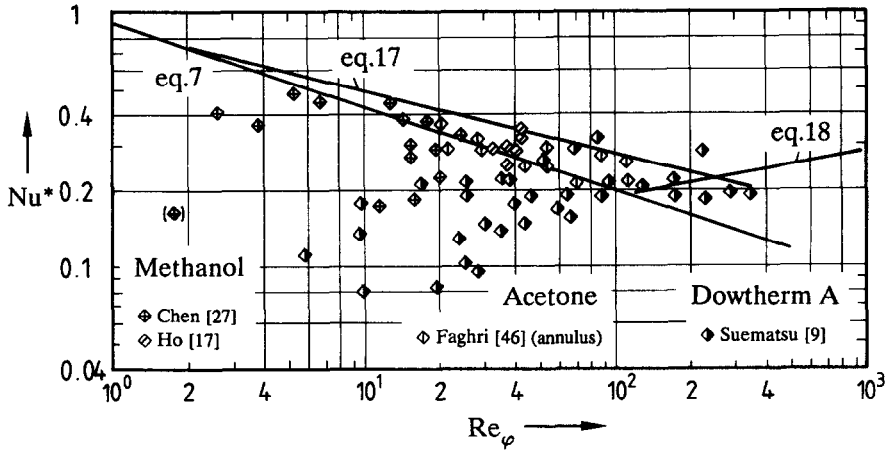

FIG. 2. Reflux condensation heat transfer with methanol, acetone and Dowtherm A.

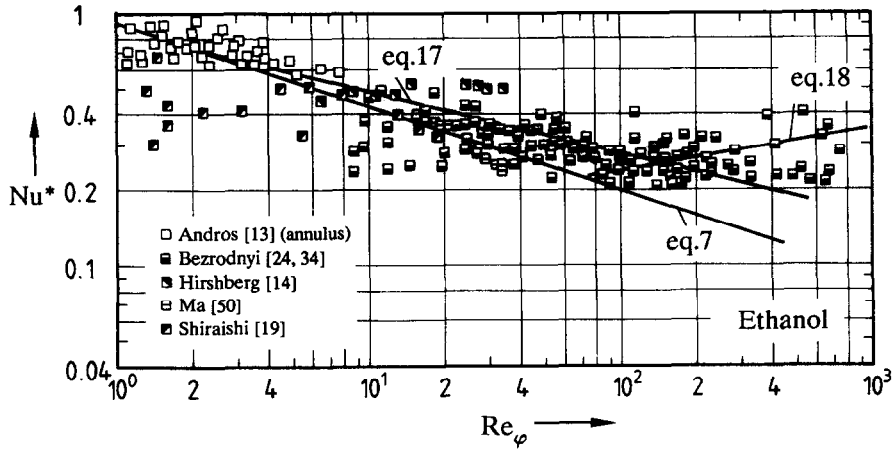

FIG. 3. Reflux condensation heat transfer with ethanol.

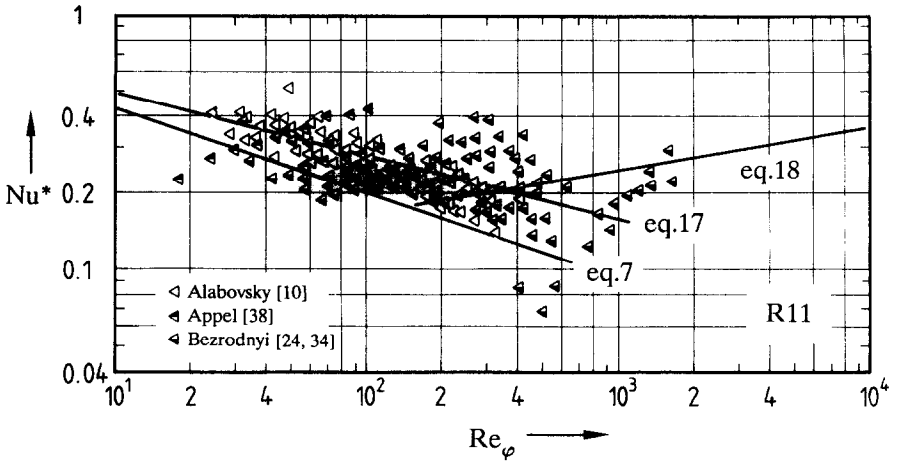

FIG. 4. Reflux condensation heat transfer with R11.

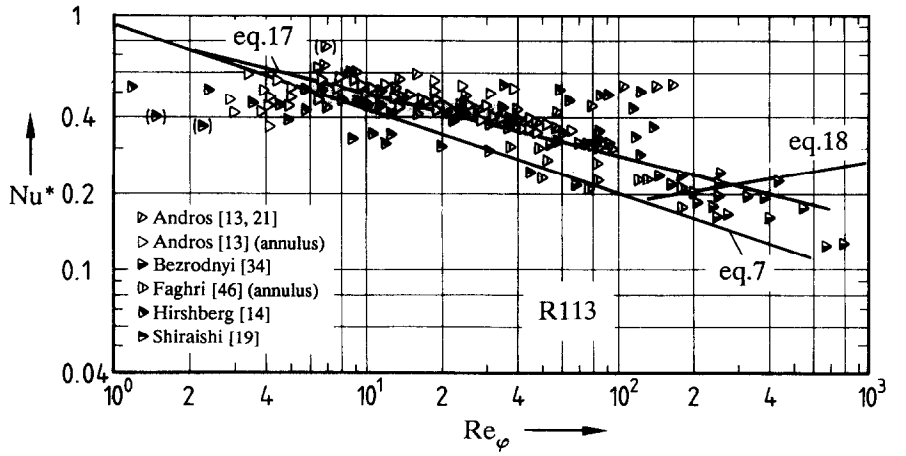

FIG. 5. Reflux condensation heat transfer with R113.

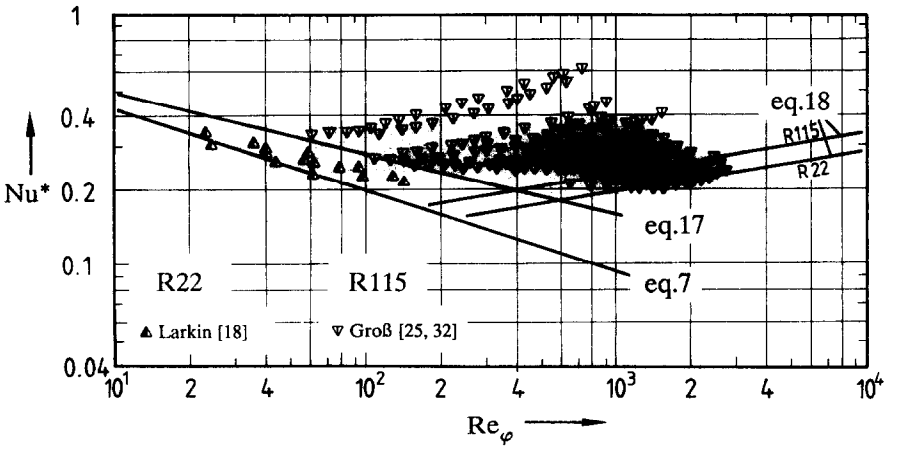

FIG. 6. Reflux condensation heat transfer with R22 and R115.

transfer measurements is usually due to uncertainties in the measurement of temperature differences, especially if they are small. All the data points have been scanned with respect to the driving temperature difference in order to check such sources of uncertainty. Some points found with $\Delta T < 0.5$ K (sometimes even $\Delta T < 0.2$ K) are plotted in parentheses (Figs. 1, 2 and 5). No significant deviation from 'normal' points can be observed.

Different fluids show different behaviour. In the case of water (Fig. 1) equation (7) seems to be an upper bound to the data, which are not seldom smaller than the predicted values by almost one order of magnitude. This holds also for Dowtherm A (Fig. 2) in a similar way. The ethanol data (Fig. 3) prove to agree much better with the plotted equations, and even an indication for transition to turbulence can be observed. R11 (Fig. 4) shows a similar behaviour, however quite a lot of data points from refs. [24, 34] are obtained above equation (17). The results with R113 clearly show, that most of the measured data follow equation (17) and exceed predicted values from equation (7) (Nusselt's theory) due to wave formation. There are again some data points, which show an extremely large enhancement of heat transfer (compared to equation (17)). The R22 data (Fig. 6) have been obtained from experiments within an almost horizontal tube ($\varphi = 85°$). They are well fitted by equation (7) in the chosen kind of diagram with Re_φ as the abscissa. Almost all of the R115 and R13B1 data (Figs. 6 and 7) are found to be well above equations (17) and (18). A deeper analysis (given in ref. [35]) pointed out that the deviations increase when the pressure is raised towards the critical point.

5.2. *Recommendation for a prediction scheme*

All the numerous experimental results can be correlated by an equation, which is based on relations well known from literature

$$Nu^* = ((f_p\, Nu^*_{eq.7})^2 + (Nu^*_{eq.18})^2)^{1/2} \qquad (19)$$

with

$$Nu^*_{eq.7} = 0.925 Re_\varphi^{-1/3}$$

$$Nu^*_{eq.18} = 0.044 Pr_l^{2/5}\, Re_\varphi^{1/6}$$

$$f_p = 1/[1 - 0.63 p^{*3.3}]$$

(f_p approaches unity for $p^* < 0.3$).

This correlation has been published previously by the present author in a modified form [35, 40, 41]. It is able to meet the following limiting cases:

(a) At a very small Reynolds number (order of $Re = 5$ and below) and at a pressure which is not too large ($p^* < 0.3$) the film flow is laminar with a smooth interface. This is the limiting case where equation (19) approaches equations (7) and (4) (for a vertical tube) respectively.

(b) At a very large Reynolds number the second term in equation (19) dominates, which represents turbulent film condensation heat transfer [58].

(c) In the intermediate range of Reynolds numbers, for laminar-wavy film flow, an increased heat transfer coefficient is obtained from equation (19) when compared with equation (7). This accounts for the wave effect and shows reasonable agreement with various wave factors from literature (see ref. [40]).

(d) Averaged thickness and velocity of the condensate film are smaller in an inclined, rather than in a vertical, thermosyphon if, e.g. Re (equation (1)) is kept constant. This is accounted for by application of the modified Reynolds number Re_φ (equation (8)) corresponding to the analytical solution for laminar film flow. However, Re_φ is also applied to turbulent films. The decrease of film thickness and velocity with increasing inclination from vertical, may yield to a laminarization of the film flow if Re_φ is not too far from turbulent–laminar transition. The inclination effect as described by equations (6)–(8) has been experimentally confirmed by refs. [14, 35].

(e) It has been found from my own experiments [35, 40, 41] at high pressures (up to the critical point: $0.4 < p^* < 1.0$) that condensation heat transfer coefficients increase for constant Reynolds number if the pressure is raised. This enhancement close to the critical point has been explained by an intensification of the wave formation, which is affected by viscosity and surface tension providing damping and smoothing effects, respectively. These effects diminish if the critical point is approached, as liquid viscosity decreases to a finite small value (neglecting critical anomaly) and surface tension becomes zero in the critical state. Wave formation is favoured by both of the effects yielding a complete desolution of the closed film structure. This has been visually observed [42] in a thermosyphon made from glass.

The agreement between experimental (Table 2, Figs. 1–7) and predicted heat transfer coefficients (equation (19)) is shown in Table 3 which also includes the respective information for the correlations recommended by ESDU [16] and by Uehara *et al.* [58]. Equation (19) is found to correlate almost 50% of all the data within deviations of $\pm 10\%$, whereas the number of data points outside $\pm 30\%$ is very small. The success of the ESDU correlation is worse, by far. This keeps true, if the high pressure data from refs. [32, 35] are cancelled and only data points at pressures $p < 13$ bar are evaluated (see the last three columns of Table 3).

The remaining deviations between measured and predicted (equation (19)) values are still significant: 4% of the experimental data are found to be below 50%, i.e. measured values are much smaller than predicted ones. It is also found that these strong deviations are restricted to a rather small number of experiments. There may be three main reasons for the deviations, namely the effects of:

- vapour shear stress at the film surface,
- non-condensable gases inside the thermosyphon.

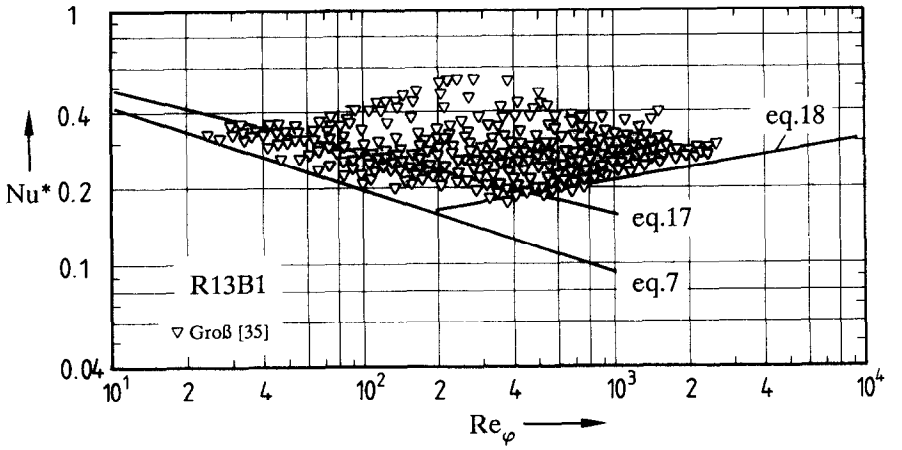

FIG. 7. Reflux condensation heat transfer with R13B1.

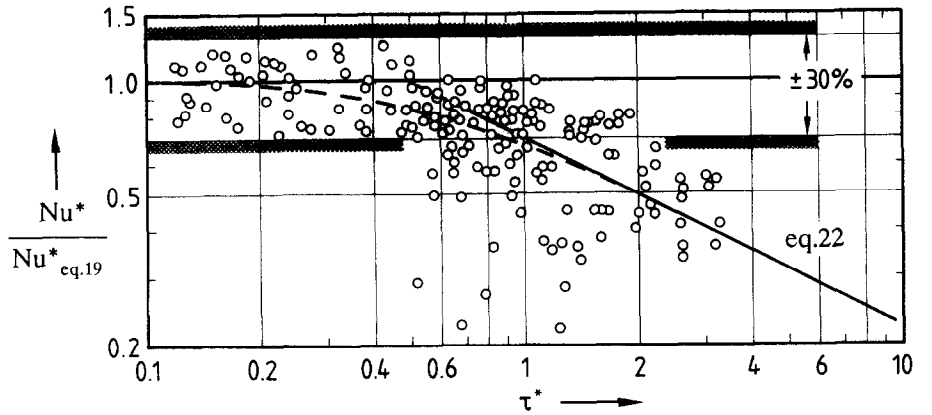

FIG. 8. Effect of the dimensionless shear stress at the liquid–vapour interface on condensation heat transfer.

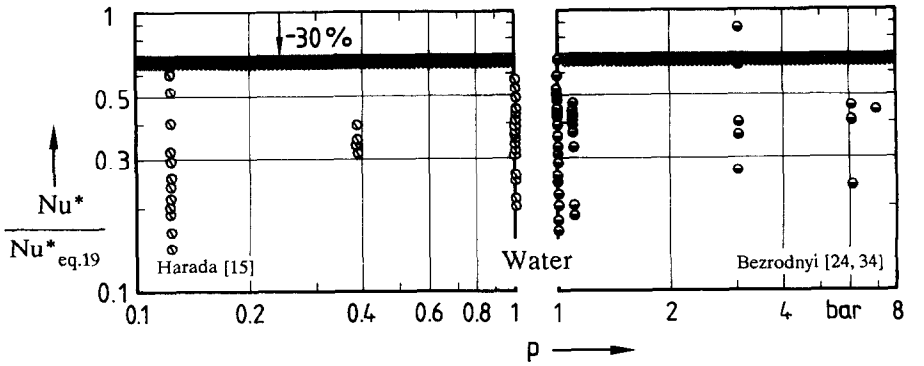

FIG. 9. Pressure effect on measured condensation heat transfer coefficients in presence of non-condensable gases (water, [15] and [24, 34]).

Table 3. Comparison between experimental and predicted condensation heat transfer coefficients inside a thermosyphon

	Present work	ESDU [16]	Uehara [58]	Present work	ESDU [16]	Uehara [58]
	equation (19)	equation (4) equation (15) equation (16)	equation (17) equation (18)	equation (19)	equation (4) equation (15) equation (16)	equation (17) equation (18)
$(\alpha_{exp}-\alpha_{pred})/\alpha_{pred}$ within	Percent of the total number of all data points			of data with $p < 13$ bar		
$\pm 10\%$	46.4	18.9	28.8	26.8	19.4	29.6
$\pm 20\%$	74.9	37.8	50.0	55.5	38.0	50.7
$\pm 30\%$	87.1	54.6	66.7	75.8	53.7	63.8
$< -50\%$	3.8	6.4	5.8	5.9	7.1	7.3
$> +50\%$	1.4	14.8	7.0	2.3	15.1	2.9

- partially flooding the cooling zone by liquid due to superfilling.

This will be analysed in the next three sections.

5.3. *Effect of vapour shear stress at the film surface*

One reason for the deviations may be due to vapour flow effects. Calculations with advanced models [27, 28, 36] brought out the impeding vapour shear effects on laminar film condensation heat transfer. The most serious effects are found with water at low temperature due to small vapour density and thus high vapour velocity. Heat transfer coefficients may decrease by 30%, depending on the assumed experimental conditions. In ref. [33] the vapour flow Froude number is assumed to be the main parameter of influence, and $Fr_{vo} = 500$ seemed to be a critical value for sensible deviations ($> 3\%$). Contradicting results are obtained from other models. In ref. [27], for example, deviations are obtained for $Fr_{vo} = 5$ which amount to 10%. So the Froude number seems to be no unique criterium for deviations.

The shear stress at the liquid–vapour interface plays the key role for vapour-flow effects on heat transfer coefficients. Following ref. [63], the shear stress between a falling liquid film and a counter current vapour flow can be expressed as

$$\tau = (\xi/8)\rho_v w_{vo}^2 \tag{20}$$

with

$$\xi = 358/\Phi^2 + 0.205/\Phi^{0.25}$$

$$\Phi = c(Re_{vo}/Re^n)(\rho_l/\rho_v)^{2/5}(\eta_v/\eta_l)^{2/3}(2\delta/d)^{1/2}$$

where

$$c = 4.76 \quad \text{and} \quad n = 3/5 \quad \text{for } Re \geqslant 40$$

$$c = 1.31 \qquad n = 1/4 \quad \text{for } Re < 40$$

and

$$\delta = 1.44\delta_v\, Re^{1/3} \qquad \text{for } Re \leqslant 516$$

$$\delta = 0.303\delta_v\, Re^{0.583} \qquad \text{for } Re > 516.$$

Finally the shear stress (equation (20)) is written dimensionless as

$$\tau^* = \tau/(g(\rho_l - \rho_v)\delta_v). \tag{21}$$

Contrary to the Froude number, equation (21) contains the effect of liquid viscosity, which must be a relevant property when falling film behaviour is studied.

Maximum shear stress arises at the locus of maximum vapour velocity, i.e. at the lower end of the cooling zone. The dimensionless shear stress τ^* has been evaluated for all the data points and it is found to be very small ($0.005 < \tau^* < 0.1$) in most of the experiments. However, there are quite a number of points where $\tau^* = 0.5$ is exceeded. Equation (19) proves to be a reasonably good correlation for the range $\tau^* < 0.5$ (agreement within $\pm 30\%$), whereas deviations grow for $\tau^* > 0.5$ with increasing shear stress. This can be observed in Fig. 8, where the ratio between measured and predicted Nusselt numbers is plotted vs τ^*. The diagram includes a total of about 200 data points taken at a large shear stress. Although the data scatter in a wide range, a significant effect of τ^* is obtained, which can be approximated for $\tau^* > 0.5$ by the following expression represented as a through-line in Fig. 8:

$$Nu^*/Nu^*_{eq.19} = (2\tau^*)^{-0.5} = 0.71/\tau^{*0.5}. \tag{22}$$

Within the entire range of shear stresses a superposition of $Nu^* = Nu^*_{eq.19}$ and equation (22) is recommended, plotted as a dashed line in Fig. 8

$$Nu^*/Nu^*_{eq.19} = (1 + 4\tau^{*2})^{-0.25}. \tag{23}$$

5.4. *Effect of non-condensable gases*

Non-condensable gases accumulate in the uppermost part of the cooling zone. They act here as an additional resistance for mass diffusion, an effect which depends on the total amount of non-condensable gases and on their local concentration.

In the course of the filling procedure of a thermosyphon tube, everything must be done to avoid non-condensable gases by repeatedly evacuating and

rinsing. The working fluid has to be degassed by freezing and evacuating before it is filled in.

However, working fluids like water and alcohols have saturation pressures pretty far below ambient pressure in a wide range of temperatures (see Table 2). Small leakages may cause penetration of air during the filling procedure and in operation. Chen *et al.* [27], for example, found from experiments with water and methanol as working fluids, that deviations from Nusselt's theory are much larger at pressures below ambient than around $p = 1$ bar (Chen's data at $p < 1$ bar cannot be evaluated here as only the pressure range has been published but not individual values). Another reason for the presence of non-condensable gases are chemical reactions between fluid and wall material, an effect which depends on temperature and time of operation. The best known reaction between the materials studied here is the water/steel reaction yielding hydrogen. In almost all the water experiments (Table 2) steel has been used as the wall material, with ref. [18] as the only exception. Age, time and kind of operation of these thermosyphons are not known, but generally the probability of a reaction increases with temperature. This could be an explanation as to why maximum deviations from theoretical predictions (Fig. 1) are observed just in experiments at elevated temperatures [9, 24, 34].

The effect of non-condensable gases has been studied intensively in a small number of investigations. Spatial distributions of vapour temperature [6] and gas concentration [43, 45] brought the idea of subdividing the vapour space into three regions: pure inert gas atop, followed by a mixing zone with concentration gradients, which are strong in radial but weak in axial direction, and finally, pure vaporized working fluid below. The most simple theoretical models are one-dimensional (axial) neglecting the mixing zone. The pressure effect on the expansion of the inert gas region is then calculated (e.g. in ref. [6]). There are advanced concepts considering the effects of mass transfer inside the mixing zone due to molecular diffusion in the presence of a laminar vapour flow [31, 47, 64, 65]. However, the vapour flow is rather turbulent than laminar in practice. Therefore, Takuma *et al.* [29] studied numerically the mass transfer behaviour in the case of a turbulent vapour flow. As a result they obtained a significant effect of heat flow (i.e. an effect of vapour Reynolds number Re_{vo}) on both mass and heat transfer. This is not a new experience. Renker [66] observed the same effect in cocurrent condensation and he suggested an equation which includes the ratio between the partial pressures of the components and additionally the vapour flow Reynolds number Re_{vo}.

Now back to the results from thermosyphon experiments. Looking to Figs. 1–7 one can observe deviations between measured and predicted Nu^* which seem to be most serious for water. There should be a pressure effect, but it cannot be found due to the limited number of experimental data. In ref. [9] pressure is not given, it is constant ($p = 1$ bar) in ref. [27], and the results in refs. [18, 19] should stay out of consideration due to uncertain accuracy of the measurements. The remaining results of Bezrodnyi and Moklyak [24, 34] and Harada *et al.* [15] do not correlate with the pressure: the deviation between measured and predicted data, plotted in Fig. 9, shows a wide range of scatter, but not a distinct pressure effect. However, at a constant pressure the deviations decrease monotonically if heat flow rate is increased. This is shown in Fig. 10 where $Nu^*/Nu^*_{eq.19}$ vs Re_{vo} is plotted.

Reynolds number indicates a mostly turbulent vapour flow ($Re_{vo} > 2300$) and may thus serve as a measure for turbulent mass transfer and the resulting mixing effect. Deviations between measured and predicted results decrease if Re_{vo} is raised (Fig. 10) as indicated by straight lines with a slope of $n = 0.5$. This behaviour has been found for various fluids in the experiments done by two other authors: Suematsu *et al.* [9] with water and Dowtherm A (Fig. 11), Andros [13] with R113 and ethanol in an annular thermosyphon (Fig. 12).

There are some reasons to assume the existence of a critical Reynolds number ($Re_{vo,trans}$), above which deviations between experiment and prediction diminish. Figure 12 especially supports this idea (Re_{vo} is calculated by means of the hydraulic diameter of the annulus). The deviations are approximately proportional to $Re_{vo}^{0.5}$ in the range below $Re_{vo,trans}$. The actual value of $Re_{vo,trans}$ varies from data set to data set but mostly it ranges around $10^4 < Re_{vo,trans} < 2 \times 10^4$. The maximum value is found in case of Harada *et al.*'s data [15] ($Re_{vo,trans} = 10^5$, if extrapolation according to $Re_{vo}^{0.5}$ is applied) and the minimum in the annular-thermosyphon experiments [13] with R113 and ethanol (as listed in Table 4).

Further evaluation of the non-condensable gas effects based on the available material does not seem to be sensible as the actual gas concentration has not been reported in all the publications on heat transfer.

5.5. *Effect of partially flooding the cooling zone due to superfilling*

In general the mass of fluid filled into a thermosyphon has no effect on cooling-zone fluid flow and heat transfer. However, this is no longer valid if the level of the two-phase mixture in the lower part of the thermosyphon is raised above the heating zone. This may be due to:

(a) superfilling or

(b) an increase of void fraction inside the two-phase mixture in the lower part of the thermosyphon.

Depending on the length of an adiabatic section, the liquid level may rise into the cooling zone [11, 13, 14, 36, 39]. In this situation filmwise condensation is restricted on the remaining vapour space above the level. In the flooded part of the cooling zone, condensation may only occur inside the vapour

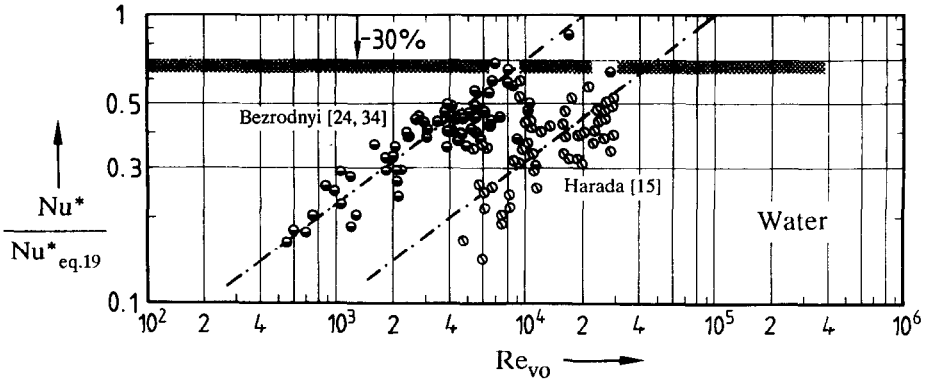

FIG. 10. Effect of vapour flow Reynolds number on condensation heat transfer coefficients in presence of non-condensable gases (water, [15] and [24, 34]).

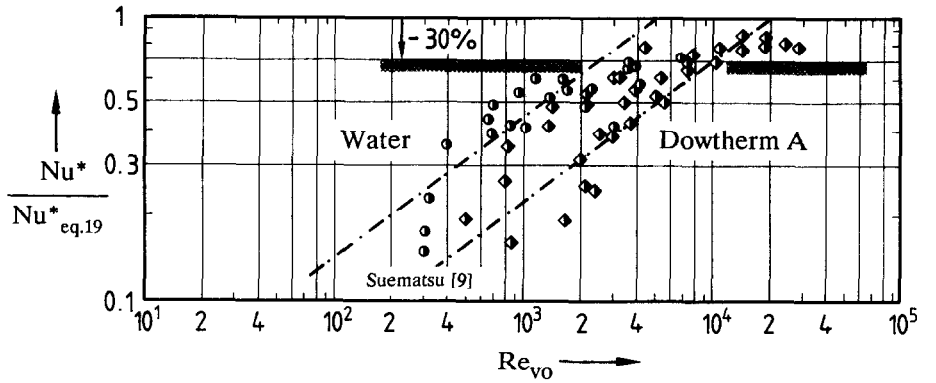

FIG. 11. Effect of vapour flow Reynolds number on condensation heat transfer coefficients in presence of non-condensable gases (water and Dowtherm A, [9]).

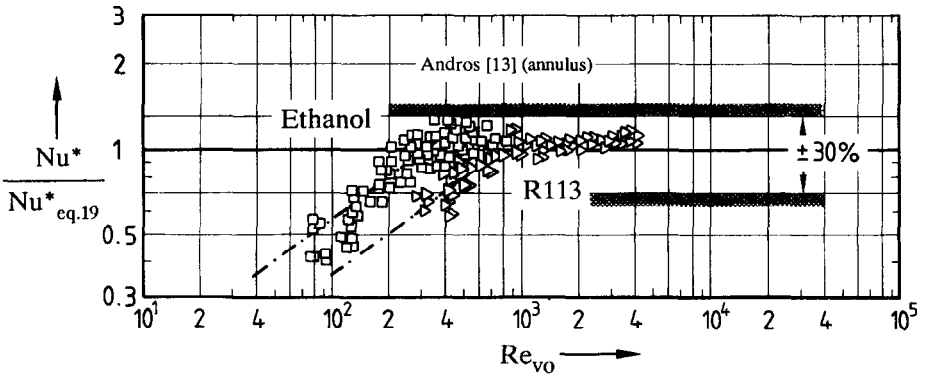

FIG. 12. Effect of vapour flow Reynolds number on condensation heat transfer coefficients in presence of non-condensable gases (R113 and ethanol, [13], annular thermosyphon).

Table 4. Critical vapour flow Reynolds number as an upper limit for non-condensable effects on condensation heat transfer as measured in the thermosyphon experiments

Author	Working fluid	$Re_{vo,trans}$	Remarks
[9]	water	5000	assumed $t_s = 100°C$
	Dowtherm A	20000	assumed $t_s = 300°C$
[13]	ethanol	300	annulus $d = d_{hydr}$
	R113	800	annulus $d = d_{hydr}$
[15]	water	100000	by extrapolation
[24, 34]	ethanol	5000	
	water	20000	
	R11	15000	
[27]	methanol	10000	

bubbles coming from below. An additional effect in an inclined tube is due to surging liquid which is free of vapour bubbles. Local temperature measurements [3, 18] brought strongly impeding effects on heat transfer.

The deviations in Figs. 1–7 may be partly due to such flooding effects. Superfilling occurs in some of the experiments in refs. [24, 34] with water, ethanol, R11 and in refs. [13, 14] with ethanol and R113. In such situations Nusselt's theory is no longer applicable and one wonders at the measured heat transfer coefficients, which are of the same order as those in filmwise condensation. The respective ethanol, R11 and R113 data are found in the upper part of the scatter (to some amount above equation (17) in Figs. 3–5), whilst the water data are below equation (17).

Andros [13] suspected "enhanced condensation below the level with the effect that less vapour is available for filmwise condensation": thickness of the film would then decrease and heat transfer coefficients increase. The idea behind this statement has not been discussed in detail. Fraction and distribution of void seem to be essential for heat transfer, with large coefficients if the liquid film remaining between a rising bubble and the cooled wall is thin.

Bezrodnyi and Moklyak [24, 34] suggest two correlations for the case of partial flooding of the cooling zone

$$Nu^* = 0.1 Pr_l^{0.54} \quad 0.04 < Fr_b(\rho_v/\rho_l) < 1.5 \quad (24)$$

$$Nu^* = 0.07 Pr_l^{0.54} (Fr_b(\rho_v/\rho_l))^{0.24} \quad 1.5 < Fr_b(\rho_v/\rho_l) < 2.5 \quad (25)$$

with the Froude number for bubbly flow $Fr_b = w_{vo}^2/(gd_b)$. No detailed investigations are reported for this case. The exact position of the two-phase level is not given in refs. [24, 34], nor any information whether the mode of operation was stationary or the process of flooding was periodical.

Anyway, flooding of the cooling zone has to be avoided if ever possible. There is no need for superfilling the tube.

6. CONCLUSIONS

A correlation (equation (19)) is suggested for the prediction of condensation heat transfer inside a thermosyphon. Shear stress effects due to vapour flow may be neglected in the range $\tau^* < 0.5$ (see equations (20) and (21)). If the dimensionless shear stress exceeds $\tau^* = 0.5$, the recommended correlation should be supplemented by an additional factor (equations (22) and (23)) which considers the deterioration of heat transfer. Special care is required to avoid non-condensable gases.

REFERENCES

1. B. S. Larkin, Heat transfer in a two-phase thermosyphon tube, *Q. Bull. Div. Eng. Natn. Aeronaut. Establ.*, Ottawa No. 3, 45–53 (1967).
2. N. M. Stoyanov, Effect of the angle of inclination of a closed evaporative thermosyphon on heat transfer, *Teploenergetika* **15**(3), 74–76 (1968).
3. B. S. Larkin, An experimental study of the two-phase thermosyphon tube, *Trans. CSME* **14**, No. B-6 (1971).
4. S. P. Andreev, A study of boiling and condensation in a heat transfer element, *Inzh. fiz. Zh.* **22**(6), 999–1005 (1972).
5. S. P. Andreev, Investigating heat transfer with phase transitions of liquid in a closed channel, *Teploenergetika* **19**(7), 88–89 (1972).
6. Z. R. Gorbis and G. A. Savchenkov, An investigation of the effect of noncondensables on the effectiveness of heat transfer of an evaporative thermosyphon, *Teploenergetika* **20**(10), 70–73 (1973).
7. D. Japikse, Advances in thermosyphon technology, *Adv. Heat Transfer* **9**, 1–111 (1973).
8. M. G. Semena and Yu. F. Kiselev, Study on heat transfer in the condensation part of two-phase thermosiphons, *Teploobmen Energ. Ustanovkakh* 68–74 (1978).
9. H. Suematsu, K. Harada, S. Inoue, J. Fujita and Y. Wakiyama, Heat transfer characteristics of heat pipes, *Heat Transfer—Jap. Res.* **7**(1), 1–22 (1978).
10. A. N. Alabovsky, M. K. Bezrodnyi and V. F. Moklyak, Study of vapour condensation heat transfer in vertical thermosyphons, *Izv. VUZav Energetika* No. 7, 61–67 (1979).
11. H. Imura, H. Kusuda, J. Ogata, T. Miyazaki and N. Sakamoto, Heat transfer in two-phase closed-type thermosyphons, *Trans. JSME* **45**(393), Ser. B, 712–722 (1979) and *Heat Transfer—Jap. Res.* **8**(2), 41–53 (1979).
12. I. G. Kiselev, A. I. Isakeev, V. V. Filatov and N. I. Istomin, Boiling and condensation in two-phase thermosiphons, *Kipenie Kondens.* **3**, 74–83 (1979).
13. F. E. Andros, Heat transfer characteristics of the two-phase closed thermosyphon (wickless heat pipe) including direct flow observations, Ph.D. Thesis, Arizona State University, Tempe (1980).
14. R. L. Hirshberg, Laminar film flow phenomena—theory and application to the two-phase thermosyphon, Ph.D. Thesis, Arizona State University, Tempe (1980).
15. K. Harada, S. Inoue, J. Fujita, H. Suematsu and Y. Wakiyama, Heat transfer characteristics of large heat pipes, *Hitachi Zosen Giho* **41**(3), 167–174 (1980).
16. ESDU, *Heat Pipes—Performance of Two-phase Closed Thermosyphons.* Engineering Sciences Data Unit 81038, London (1981).
17. W. K. Ho and C. L. Tien, Reflux condensation characteristics of a two-phase closed thermosyphon, *Proc. 4th Int. Heat Pipe Conf.*, London, pp. 451–458 (1981).
18. B. S. Larkin, An experimental study of the temperature profiles and heat transfer coefficients in a heat pipe for

a heat exchanger, *Proc. 4th Int. Heat Pipe Conf.*, London, pp. 177–191 (1981).
19. M. Shiraishi, K. Kikuchi and T. Yamanishi, Investigation of heat transfer characteristics of a two-phase closed thermosyphon, *Proc. 4th Int. Heat Pipe Conf.*, London, pp. 95–104 (1981).
20. Th. Spendel, Laminar film condensation heat transfer in closed two-phase thermosiphons, *Proc. 4th Int. Heat Pipe Conf.*, London, pp. 163–173 (1981).
21. F. E. Andros and L. W. Florschuetz, Heat transfer characteristics of the two-phase closed thermosyphon (wickless heat pipe), *Proc. 7th Int. Heat Transfer Conf.*, Munich, Vol. 4, pp. 187–192 (1982).
22. N. I. Mirmov, V. D. Portnov and I. G. Belyakova, Study of the heat transfer coefficient during vapor condensation in thermosiphons, *Izv. VUZav Energetika* No. 7, 100–103 (1982).
23. M. Takuma, S. Maezawa and A. Tsuchida, Studies on condensation heat transfer in two-phase closed thermosyphons, *Proc. Symp. Mech. Space Flight*, pp. 247–255 (1982).
24. M. K. Bezrodnyi and V. F. Moklyak, Heat transfer during condensation in a dynamic two-phase layer of closed thermosiphons, *Izv. VUZav Energetika* No. 4, 99–105 (1983).
25. U. Groß, Der Wärmeübergang in einem geschlossenen Thermosyphon, der Fluid nahe dem thermodynamisch kritischen Zustand enthält, Doctoral Dissertation, Universität Stuttgart (1983).
26. N. I. Mirmov and I. G. Belyakova, Heat liberation during vapor condensation in a thermosiphon, *Inzh. fiz. Zh.* **43**(3), 385–390 (1982).
27. S. J. Chen, J. G. Reed and C. L. Tien, Reflux condensation in a two-phase closed thermosyphon, *Int. J. Heat Mass Transfer* **27**, 1587–1594 (1984).
28. R. A. Seban and A. Faghri, Film condensation in a vertical tube with a closed top, *Int. J. Heat Mass Transfer* **27**, 944–948 (1984).
29. M. Takuma, S. Maezawa and A. Tsuchida, Effects of turbulent diffusion on thermal characteristics of a gas-loaded two-phase closed thermosyphon, *Proc. 5th Int. Heat Pipe Conf.*, Tokyo, Vol. 1, pp. 232–239 (1984).
30. Th. Spendel, Laminar film condensation heat transfer in closed two-phase thermosyphons, *Proc. 5th Int. Heat Pipe Conf.*, Tokyo, Vol. 1, pp. 208–213 (1984).
31. K. Hijikata, S. J. Chen and C. L. Tien, Non-condensable gas effect on condensation in a two-phase closed thermosyphon, *Int. J. Heat Mass Transfer* **27**, 1319–1325 (1984).
32. U. Groß and E. Hahne, Heat transfer in a two-phase thermosyphon operating with a fluid in the near critical state, *Int. J. Heat Mass Transfer* **28**, 589–601 (1985).
33. Th. Spendel, Laminare Filmkondensation im vertikalen geschlossenen Zweiphasen-Thermosiphon, Doctoral Dissertation, Universität Stuttgart (1985).
34. M. K. Bezrodnyi and V. F. Moklyak, Heat transfer in condensation in vertical closed thermosiphon, *Inzh. fiz. Zh.* **51**(1), 9–16 (1986).
35. U. Groß and E. Hahne, Reflux condensation inside a two-phase thermosyphon at pressures up to the critical, *Proc. 8th Int. Heat Transfer Conf.*, San Francisco, pp. 1613–1620 (1986).
36. M. Takuma, S. Maezawa and A. Tsuchida, Condensation heat transfer characteristics of the annular two-phase closed thermosyphon, *Nippon Kikai Gakkai Ronbunshu, B-hen* **52**(482), 3537–3544 (1986).
37. M. Xin and J. Xia, Heat transfer by dropwise condensation in the two-phase closed thermosiphons, *Proc. 8th Int. Heat Transfer Conf.*, San Francisco, Vol. 4, pp. 1683–1688 (1986).
38. G. Appel, Experimentelle und theoretische Untersuchung zur Leistungscharakteristik von Gravitationswärmerohren, *Fortschr. Ber. Ver. dt. Ing.* Ser. 6, No. 195 (1987), also Doctoral Dissertation, Universität der Bundeswehr, Munich (1987).
39. Y. Ma, J. Liu and Y. Fung, The characteristics of condensation heat transfer in thermosyphons, *Proc. 6th Int. Heat Pipe Conf.*, Grenoble, Vol. 3, pp. 445–450 (1987).
40. U. Groß und E. Hahne, Experimentelle Untersuchung des Wärmeüberganges bei der Rückstrom-Kondensation in einem geneigten Rohr, *Chemie-Ingr-Tech.* **59**, 168–169 (1987).
41. U. Groß and E. Hahne, Condensation heat transfer inside a closed thermosyphon—generalized correlation of experimental data, *Proc. 6th Int. Heat Pipe Conf.*, Grenoble, Vol. 3, pp. 466–471 (1987).
42. E. Hahne, U. Groß und G. Barthau, Optische Erscheinungen im thermodynamisch kritischen Gebiet—Beobachtung und Deutung der Vorgänge in einem Thermosyphon, *Wärme- und Stoffübertragung* **21**, 155–162 (1987).
43. Y. Kobayashi and T. Matsumoto, Vapor condensation in the presence of non-condensable gas in the gravity assisted thermosyphon, *Proc. 6th Int. Heat Pipe Conf.*, Grenoble, Vol. 3, pp. 413–418 (1987).
44. S. Rösler and M. Groll, Measurement of the condensate film structure in closed two-phase thermosyphons, *Proc. 6th Int. Heat Pipe Conf.*, Grenoble, Vol. 3, pp. 441–444 (1987).
45. P. F. Peterson and C. L. Tien, Gas-concentration measurements and analysis for gas-loaded thermosyphons, *J. Heat Transfer* **110**, 743–747 (1988).
46. A. Faghri, M.-M. Chen and M. Morgan, Heat transfer characteristics in two-phase closed conventional and concentric annular thermosyphons, *J. Heat Transfer* **111**, 611–618 (1989).
47. P. F. Peterson and C. L. Tien, Numerical and analytical solutions for two-dimensional gas distribution in gas-loaded heat pipes, *J. Heat Transfer* **111**, 598–604 (1989).
48. A. S. Assad and S. V. Konev, Analysis of condensation in small cross sectional thermosyphons, Prepr. 7th Int. Heat Pipe Conf., Minsk (1990).
49. F. M. Gerner and C. L. Tien, Effects of high interfacial shear stress due to countercurrent vapor flow on film condensation heat transfer, Prepr. 7th Int. Heat Pipe Conf., Minsk (1990).
50. T. Ma, H. Wei, H. Chen and S. Zhang, Condensation heat transfer in vertical two-phase closed thermosyphon, Prepr. 7th Int. Heat Pipe Conf., Minsk (1990).
51. A. Niro, G. Radaelli and P. A. Andreini, Heat transfer characteristics in a closed two-phase thermosyphon, *Proc. 9th Int. Heat Transfer Conf.*, Jerusalem, Vol. 2, pp. 81–86 (1990).
52. O. Tanaka, H. Koshino, H. Sakai, R. Furukawa and Y. Inada, Heat transfer characteristics of super heat pipes, Prepr. 7th Int. Heat Pipe Conf., Minsk (1990).
53. T. Fukano, K. Kadoguchi and C. L. Tien, Local heat transfer in a reflux condensation inside a closed two-phase thermosyphon, *Proc. 9th Int. Heat Transfer Conf.*, Jerusalem, Vol. 3, pp. 85–90 (1990).
54. Z. Sun, Y. Zhao and Y. Zhang, Analysis and calculation of condensation heat transfer procedure of two-phase closed thermosyphon, Prepr. 7th Int. Heat Pipe Conf., Minsk (1990).
55. P. F. Peterson, N. Elkouh, K. W. Lee and C. L. Tien, Flow instability and bifurcation in gas-loaded reflux thermosyphons, *J. Heat Transfer* **113**, 158–165 (1991).
56. X. Zhou and R. E. Collins, Measurement of condensation heat transfer in a thermosyphon, *Int. J. Heat Mass Transfer* **34**, 369–376 (1991).
57. U. Groß, Kondensation und Verdampfung im geschlossenen Thermosyphon, *Fortschr. Ber. Ver. dt. Ing.* Ser. 19, No. 46 (1991).
58. H. Uehara, H. Kusuda, T. Nakaoka and M. Yamada, Filmwise condensation for turbulent flow on a vertical plate, *Heat Transfer—Jap. Res.* **12**(2), 85–96 (1983).

59. W. Nusselt, Die Oberflächenkondensation des Wasserdampfes, *Z. Ver. dt. Ing.* **60,** 541–546 and 569–575 (1916).
60. K. E. Hassan and M. Jakob, Laminar film condensation of pure saturated vapours on inclined circular cylinders, ASME Paper No. 57-A-35 (1957).
61. W. H. Henstock and T. J. Hanratty, The interfacial drag and the height of the wall layer in annular flows, *A.I.Ch.E. Jl* **22,** 990–1000 (1976).
62. H. Imura, K. Sasaguchi, H. Kozai and S. Numata, Critical heat flux in a closed two-phase thermosyphon, *Int. J. Heat Mass Transfer* **26,** 1183–1188 (1983).
63. H. Brauer, *Grundlagen der Einphasen- und Mehrphasenströmungen*. Sauerländer, Aarau and Frankfurt (1971).
64. B. D. Marcus, Theory and design of variable conductance heat pipes, NASA CR-2018 (April 1972).
65. A. R. Rohani and C. L. Tien, Steady two-dimensional heat and mass transfer in the vapour–gas region of a gas-loaded heat pipe, *J. Heat Transfer* **95,** 377–382 (1973).
66. W. Renker, Der Wärmeübergang bei der Kondensation von Dämpfen in Anwesenheit nicht kondensierbarer Gase, *Chemie Techn.* **7,** 451–461 (1955).

TRANSFERT THERMIQUE DE CONDENSATION DANS UN THERMOSYPHON FERME

Résumé—On examine le transfert thermique de condensation dans un thermosyphon biphasique et on fait une description détaillée de l'écoulement du fluide, ainsi qu'une revue des études expérimentales et théoriques. On a évalué 18 travaux de recherche et traité 2889 points de mesure couvrant des larges domaines des paramètres thermiques et géométriques: 10 fluides de travail différents, température de saturation ($14°C \leqslant t_s \leqslant 340°C$), pression ($0{,}04 \leqslant p \leqslant 39{,}5$ bar), diamètre intérieur du tube ($14 \leqslant d \leqslant 66$ mm), longueur de la zone réfrigérante ($102 \leqslant L \leqslant 2450$ mm), et l'angle d'inclinaison ($0° \leqslant \varphi \leqslant 85°$). Des formules sont proposées pour les transferts thermiques de condensation dans un thermosyphon biphasique. Les déviations constatées sont dues aux effets du cisaillement à l'interface liquide-vapeur, des gaz incondensables et du reflux partiel dans la zone froide dans le cas d'un remplissage excessif du thermosyphon.

WÄRMEÜBERGANG BEI RÜCKSTROM-KONDENSATION IM GESCHLOSSENEN THERMOSYPHON

Zusammenfassung—In der vorgelegten Arbeit wird der Wärmeübergang bei Kondensation in einem Zweiphasen-Thermosyphon analysiert und beschrieben. Grundlage dafür bilden die zahlreich in der Literatur vorhandenen experimentellen und theoretischen Untersuchungen. Sämtliche in der zugänglichen Literatur verfügbaren und auswertbaren Versuchsergebnisse für den Wärmeübergang werden gesammelt und geordnet. Aus 18 Arbeiten wurden 2889 Versuchspunkte entnommen, die weite Parameterbereiche abdecken: 10 unterschiedliche Arbeitsfluide, Sättigungstemperatur ($14°C \leqslant t_s \leqslant 340°C$), Druck ($0{,}04 \leqslant p \leqslant 39{,}5$ bar), Innendurchmesser und Länge der Kühlzone ($14 \leqslant d \leqslant 66$ mm; $102 \leqslant L \leqslant 2450$ mm), Neigungswinkel ($0° \leqslant \varphi \leqslant 85°$). Es wird eine Berechnungsgleichung für den Wärmeübergang bei Kondensation vorgeschlagen, die gut mit den Versuchsdaten korreliert. Verbleibende Abweichungen werden auf den Einfluß der Schubspannung an der Filmoberfläche infolge der Gegenströmung von Dampf, auf nicht-kondensierbare Gase sowie auf eine partielle Überflutung der Kühlzone bei Wahl einer zu großen Füllmenge zurückgeführt.

ТЕПЛОПЕРЕНОС ПРИ КОНДЕНСАЦИИ В ЗАМКНУТОМ ТЕРМОСИФОНЕ

Аннотация—Дается анализ теплопереноса при конденсации в двухфазном термосифоне, включающий подробное онисание течения жидкости, а также обзор опубликованных экспериментальных и теоретических исследований. Приводятся результаты для 2889 реперных точек, полученные в 18 исследовательских работах, для следующих широких диапазонов тепловых и геометрических параметров: 10 различных рабочих жидкостей, температцры насыщения $14°C \leqslant t_s \leqslant 340°C$, давления $0{,}04 \leqslant p \leqslant 39{,}5$ бар, внутреннего диаметра трубы $14 \leqslant d \leqslant 66$ мм, длины зоны охлаждения $102 \leqslant L \leqslant 2450$ мм и угла наклона $0° \leqslant \varphi \leqslant 85°$. Предложены обобщающие соотношения для теплопереноса при конденсации в двухфазном термосифоне. Расхождения обусловлены следующими эффектами: касательного напряжения на границе раздела жидкостьпар, неконденсирующихся газов и частичного затопления зоны охлаждения в случае переполнения термосифона.